

Giant in-plane anisotropy in manganite thin films driven by strain-engineered double exchange interaction and electronic phase separation

C. L. Lu,^{1,2,a)} Y. Y. Wu,³ Z. C. Xia,³ S. L. Yuan,¹ L. Chen,¹ Z. M. Tian,¹ J.-M. Liu,^{4,5} and T. Wu^{2,a)}

¹School of Physics, Huazhong University of Science and Technology, Wuhan 430074, China

²Division of Physics and Applied Physics, School of Physical and Mathematical Sciences, Nanyang Technological University, Singapore 637371, Singapore

³Wuhan National High Magnetic Field Center, Huazhong University of Science and Technology, Wuhan 430074, China

⁴Laboratory of Solid State Microstructure, Nanjing University, Nanjing 210093, China

⁵International Center for Materials Physics, Chinese Academy Sciences, Shenyang 110016, China

(Received 31 July 2011; accepted 4 September 2011; published online 23 September 2011)

We investigate epitaxial $\text{Pr}_{0.65}(\text{Ca}_{0.7}\text{Sr}_{0.3})_{0.35}\text{MnO}_3$ thin film grown on orthorhombic (110) NdGaO_3 substrate which breaks the lattice symmetry and affects the phase separated ground state. As a result of the anisotropic substrate strain, giant in-plane magnetic and magnetotransport anisotropy are observed, which is related to the anisotropic coupling and competition between the double-exchange interaction and the Jahn-Teller distortion. Furthermore, the in-plane anisotropy shows a distinct enhancement near the metal-insulator transition, implying a significant contribution from the phase separation to the anisotropic transport behaviors. © 2011 American Institute of Physics. [doi:10.1063/1.3643442]

Since the discovery of “colossal magnetoresistance” (CMR),^{1–3} perovskite manganites have drawn significant attention due to both the fundamental science and the potential applications. In these materials, the complex and strong coupling between spin, charge, orbital, and lattice degrees of freedom gives rise to multiple competing phases with essentially distinct physical properties. Moreover, these phases are quite “soft” in the sense that their free energies are close to each other, thus forming a delicate balance which is very sensitive to internal/external perturbations, such as electric field (current),^{4,5} light,⁶ phonon,⁷ and strain,^{8–13} in addition to magnetic field. Among these tuning parameters, strain stands out as it is ubiquitous in thin films and devices, and it has been shown that strain also can significantly affect the charge, spin, and orbital orders in manganite thin films.^{14–18}

The physical properties of manganite thin films can be modulated over a wide range by strain from the underlying substrates,^{8–14} and one of the most cited mechanisms is the strain mediated orbital-ordering of the e_g state, which couples with the Jahn-Teller (JT) distortion of the MnO_6 octahedra.¹⁹ Recently, substrate strain has been engineered to give rise to in-plane (IP) anisotropic magnetism and transport behaviors.²⁰ Furthermore, the effects of anisotropic strain in manganite thin films have been discussed from both experimental^{21,22} and theoretical²³ perspectives. A significant IP uniaxial magnetic anisotropy was reported in ferromagnetic (FM) metallic $\text{La}_{2/3}\text{Sr}_{1/3}\text{MnO}_3$ (LSMO) thin films, suggesting that phase separation (PS) is not a prerequisite for observing anisotropic properties.^{21,22} Recently, Dong *et al.*²³ theoretically revealed that the anisotropic double-exchange (DE) interaction and JT distortions were the most important ingredients for the highly IP anisotropic behaviors in strained manganite thin films.

Clearly, the complex physics involving anisotropy in manganite thin films warrants further in-depth investigations.

In this letter, we address this issue by studying in details the structure, magnetism, and magnetotransport behaviors of $\text{Pr}_{0.65}(\text{Ca}_{0.7}\text{Sr}_{0.3})_{0.35}\text{MnO}_3$ (PCSMO) thin film epitaxially grown on (110) NdGaO_3 (NGO) substrate. PCSMO is a typical PS manganite with coexisting and competing charge-ordered (CO) and FM phases. Our results reveal giant IP magnetic and transport anisotropy in the film, which can be associated with the anisotropic coupling and competition between the DE interaction and the JT distortion. Importantly, the observation of strain effects which are amplified by the electronic phase separation puts constraints on the potential theoretical models that can be used to elucidate the physics of competing energetics in complex oxides.

PCSMO thin films with a thickness of 80 nm were epitaxially deposited on (110) NGO substrates using pulsed laser deposition (PLD) at 750 °C in 150 mTorr oxygen. A KrF excimer laser ($\lambda = 248$ nm) was used with an energy density of ~ 1.3 J/cm² and a repetition rate of 3 Hz. The topographic imaging measurement was carried out on an atomic force microscope (AFM) (Asylum Research, MFP-3D). The crystalline structure of the film was examined using a high-resolution x-ray diffraction (HRXRD) system. Magnetic properties as a function of temperature (T) and magnetic field (H) were measured using a quantum design magnetic properties measurement system (MPMS). The magnetotransport behaviors were measured using a standard four-probe method in a quantum design physical property measurement system (PPMS).

Fig. 1(a) presents the HRXRD pattern of PCSMO/NGO thin film. The pure c -axis orientation indicates the good crystallinity and epitaxy of the film. The pseudocubic PCSMO has lattice parameters $a = 3.851$ Å, $b = 3.840$ Å, and $c = 3.848$ Å,¹² while NGO substrate has an orthorhombic crystalline structure with lattice parameters $a = 5.43$ Å,

^{a)}Authors to whom the correspondence should be addressed. Electronic addresses: cllu@mail.hust.edu.cn and tomwu@ntu.edu.sg.

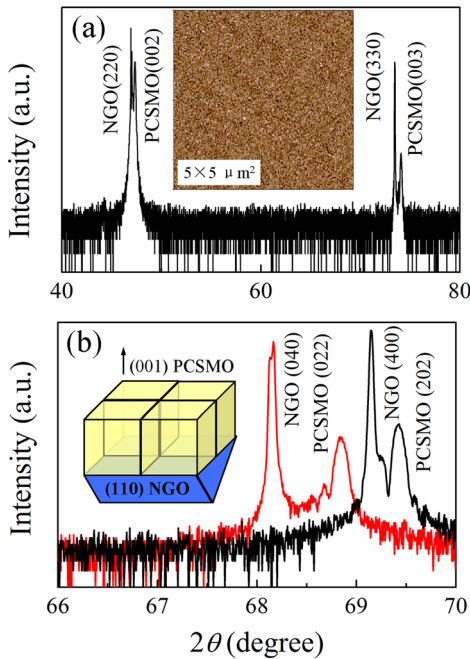


FIG. 1. (Color online) (a) Symmetric x-ray θ - 2θ scan of the PCSMO/NGO thin film, and the inset shows the $5 \times 5 \mu\text{m}^2$ topographic AFM image of the film (the height of the scale is 3 nm). (b) Asymmetric scans along the (100) and (010) of the NGO substrate, and the inset shows the schematic drawing of the epitaxial growth of PCSMO on (110) NGO.

$b = 5.50 \text{ \AA}$, and $c = 7.71 \text{ \AA}$. The out-of-plane (OOP) lattice parameter of the film was found to be $\sim 3.837 \text{ \AA}$, which is smaller than the bulk value, indicating a biaxial tensile strain ($\sim 0.4\%$). (110) NGO has IP parameters of 7.73 and 7.71 \AA , thus an “cubic-on-cubic” stacking is favored for the PCSMO growth,²¹ which is schematically shown in the inset of Fig. 1(b). To understand the IP crystalline structure of the film, the asymmetric line-scans along (100) and (010) of the substrate are presented in Fig. 1(b), and the presence of multiple internal interference peaks further confirms the uniformity and epitaxy of the film. The IP lattice parameters of the film can be estimated to be 3.871 and 3.853 \AA along [100] and [010] directions, respectively. The anisotropic strain is $\sim 0.5\%$ along [100] and $\sim 0.3\%$ along [010]. In addition, the topographic imaging reveals a very smooth surface of the film without any morphological anisotropy (inset of Fig. 1(a)), and the root mean square roughness (R_{RMS}) is about 0.5 nm, confirming the high quality of the film.

To investigate the effects of anisotropic strain on the physical properties of the PCSMO thin film, detailed magnetic and magnetotransport data were measured. The H -dependence of magnetization (M) measured along the two IP directions ([100] and [010]) at $T = 80 \text{ K}$ is shown in Fig. 2(a). A clear IP uniaxial magnetic anisotropy can be observed with the larger remnant magnetization and coercive field lying in the [100] direction, which can be taken as the easy axis. This uniaxial anisotropy was further confirmed in the M - T data, which were measured under both the zero-field-cooled (ZFC) and the field-cooled (FC) conditions with an applied field of 100 Oe. As shown in Fig. 2(b), along the [100] direction, the FC curve shows a sudden increase at $T_C \sim 126 \text{ K}$ as a result of the onset of the FM phase. The large discrepancy between the FC and ZFC curves below T_C is a signature of the low

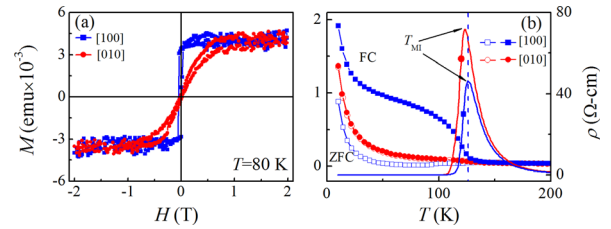


FIG. 2. (Color online) (a) Hysteresis loops of the PCSMO film measured along the two in-plane directions at $T = 80 \text{ K}$. (b) Temperature dependence of magnetization (left axis, for both the field-cooled and the zero-field-cooled conditions) and resistivity (right axis) measured along the two in-plane directions of the PCSMO film.

temperature PS in the PCSMO film.²⁴ In contrast, along the [010] direction, the FC and ZFC curves overlap with each other and no abrupt magnetic transition can be observed down to 5 K. As shown in Fig. 2(b), the T -dependent resistivity of the PCSMO film exhibits a very sharp metal-insulator transition (MIT) at T_{MI} . The transport data exhibit a clear anisotropy, i.e., T_{MI} is higher and resistivity is smaller in the [100] direction compared with those in the [010] direction, indicating that the hopping of the e_g electrons is much easier along [100]. The difference of T_{MI} under zero magnetic field between the two IP directions is about 3 K.

In order to understand the role of PS in the transport anisotropy in strained manganite films, we used magnetic fields to tune PS. As shown in Fig. 3(a), the zero field $\rho(T)$ curve exhibits a distinct hysteresis, which is often identified in manganites with PS.²⁴ The thermal hysteresis in the $\rho(T)$ curves is reduced as the applied field increases, and the values of T_{MI} during cooling and warming are very close to each other as $H > 1.6 \text{ T}$, indicating the weakening of the quenched-disorder-induced macroscopic PS. The H -dependence of T_{MI} , for both the cooling and warming processes, is plotted in Fig. 3(b). With increasing H , T_{MI} monotonously shifts toward higher T , while the difference between the cooling and warming data starts to shrink as $H > 0.5 \text{ T}$ and eventually overlap with each other at $H > 1.6 \text{ T}$, which suggests a strong suppression of the PS state at high magnetic fields. However, the gap between the values of T_{MI} measured along the two IP directions does not shrink at all up to $H = 2.5 \text{ T}$ (Fig. 3(c)), which implies that the transport anisotropy is retained even when PS is substantially suppressed. Therefore, other factors besides PS contribute to the observed giant anisotropy in strained manganite films.

The schematic drawing in Fig. 4 illustrates the emergence of uniaxially elongated FM-metallic (FMM) clusters randomly distributed in the CO insulating (COI) matrix (left part of the figure), where the anisotropic strain promotes the growth of FMM phase along the [100] direction. Thus, in the PCSMO film with PS, an anisotropic percolation at the MIT as well as the consequent response to external fields would be expected. On the other hand, to understand the physics underlying these observed anisotropic behaviors, we have to consider the strain mediated orbital properties which have been shown to play important roles in strained manganite films.^{19,23} For the unstrained pseudocubic case with a high crystalline symmetry, equal weights of different orbitals (such as $|3y^2 - r^2\rangle$ and $|3x^2 - r^2\rangle$) and uniform overlaps between electronic clouds in different directions are

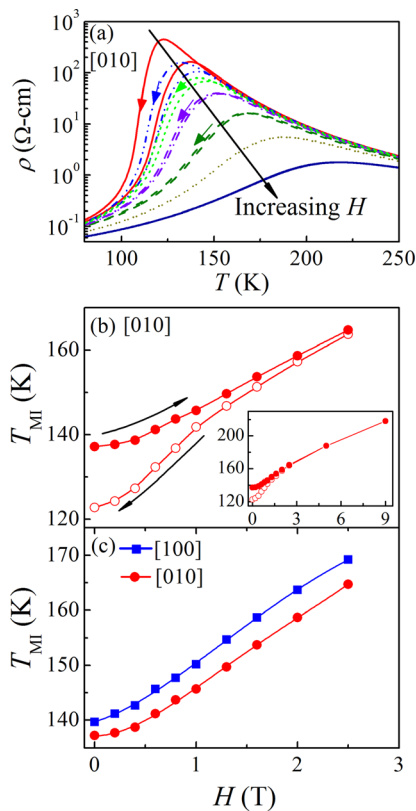


FIG. 3. (Color online) (a) T -dependence of resistivity measured along [010] direction under different magnetic field ($H = 0, 0.6, 1.0, 1.6, 2.5, 5.0, 9.0$ T). The cooling processes are indicated by arrows except for cases of $H = 5.0$ and 9.0 T, in which $\rho(T)$ curves measured during cooling and warming overlap with each other. (b) H -dependence of the metal-insulator transition temperature T_{MI} in the PCSMO film measured along the [010] direction during both cooling and warming. T_{MI} measured in a wider range of H is shown in the inset. (c) H -dependence of T_{MI} measured in both in-plane directions during warming.

expected, which lead to the isotropic DE interaction and JT distortions. Thus, identical transport and magnetic properties in different crystalline directions are expected. However, in the current case of PCSMO films grown on (110) NGO substrates, the IP anisotropic tensile strain causes different bending conditions of Mn-O-Mn bonds along two IP directions, i.e., compared to the [010] direction, the larger tensile strain along [100] gives rise to a stronger overlap of the electronic clouds (Fig. 4 (right)). Thus, the reduced bending of Mn-O-Mn bond in the [100] direction will promote the e_g electron hopping, strengthen the FM-DE interaction, and alleviate the JT distortions,^{2,25} which contribute to the observed giant IP anisotropy in PCSMO/NGO thin films.

In the theoretical study by Dong *et al.*,²³ the anisotropic double-exchange and John-Teller distortions were found to be responsible for the anisotropic transport in strained manganites. Our results on PCSMO films on (110) NGO substrates indeed reveal giant in-plane anisotropic magnetism and resistivity, giving support to the theory. Furthermore, it is clear that PS significantly contributes to the strain-induced anisotropy, and the anisotropy of physical properties is “amplified” at the phase boundary. Thus, the long range strain field is effective to not only influence the competition between separated phases, but also couple to the spin and orbital degrees of freedoms in manganite thin films.

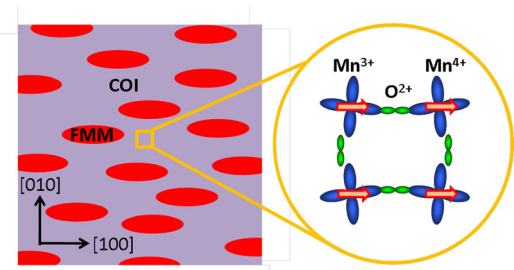


FIG. 4. (Color online) Schematic illustrating the effect of anisotropic substrate strain on the manganite films with phase separation. Left: the uniaxially elongated FMM phase within the COI matrix contributes to the observed anisotropic transport. Right: the anisotropic strain causes a stronger overlap of the Mn orbitals along the [100] direction compared to the [010] direction, which gives rise to anisotropic double-exchange and Jahn-Teller distortions.

This work was partly supported by the Singapore National Research Foundation, NSFC (Grant No. 11104090), and the Ministry of Education of China (Grant No. 309020). J.M.L. was supported by NSFC (Grant Nos. 50832002 and 11074113).

- ¹S. Jin, T. H. Tiefel, M. McCormack, R. A. Fastnacht, R. Ramesh, and L. H. Chen, *Science* **264**, 413 (1994).
- ²E. Dagotto, T. Hotta, and A. Moreo, *Science* **309**, 257 (2005).
- ³Y. Tokura, *Rep. Prog. Phys.* **69**, 797 (2006).
- ⁴H. Sakai and Y. Tokura, *Appl. Phys. Lett.* **92**, 102514 (2008).
- ⁵B. T. Xie, Y. G. Zhao, and C. M. Xiong, *Appl. Phys. Lett.* **93**, 072112 (2008).
- ⁶M. Rini, R. Tobey, N. Dean, J. Itatani, Y. Tomioka, Y. Yokura, R. W. Schoenlein, and A. Cavalleri, *Nature* **449**, 72 (2007).
- ⁷F. Maciá, A. H. Mínguez, G. Abril, J. M. Hernandez, A. G. Santiago, J. Tejada, F. Parisi, and P. V. Santos, *Phys. Rev. B* **76**, 174424 (2007).
- ⁸S. W. Jin, G. Y. Gao, Z. Z. Yin, Z. Huang, X. Y. Zhou, and W. B. Wu, *Phys. Rev. B* **75**, 212401 (2007).
- ⁹F. H. Zhang, Z. Huang, G. Y. Gao, P. F. Chen, L. F. Wang, X. L. Tan, and W. B. Wu, *Appl. Phys. Lett.* **96**, 062507 (2010).
- ¹⁰T. Wu, S. B. Ogale, S. Shinde, A. Biswas, T. Polletto, R. L. Greene, T. Venkatesan, and A. J. Millis, *J. Appl. Phys.* **93**, 5507 (2003).
- ¹¹T. Wu and J. F. Mitchell, *Appl. Phys. Lett.* **86**, 062502 (2005); *Phys. Rev. B* **74**, 214423 (2006).
- ¹²T. Wu and J. F. Mitchell, *J. Magn. Magn. Mater.* **292**, 25 (2005).
- ¹³Y. H. Sun, Y. G. Zhao, H. F. Tian, C. M. Xiong, B. T. Xie, M. H. Zhu, S. Park, W. Wu, J. Q. Li, and Q. Li, *Phys. Rev. B* **78**, 024412 (2008).
- ¹⁴Y. Q. Zhang, Z. D. Zhang, and J. Aarts, *Phys. Rev. B* **79**, 224422 (2009).
- ¹⁵J. Dho, Y. N. Kim, Y. S. Hwang, J. C. Kim, and N. H. Hur, *Appl. Phys. Lett.* **82**, 1434 (2003).
- ¹⁶A. Sadoc, B. Mercey, C. Simon, D. Grebille, W. Prellier, and M.-B. Lefpetit, *Phys. Rev. Lett.* **104**, 046804 (2010).
- ¹⁷M. Nakamura, Y. Ogimoto, H. Tamaru, M. Izumi, and K. Miyano, *Appl. Phys. Lett.* **86**, 182504 (2005); Y. Ogimoto, M. Nakamura, N. Takubo, H. Tamaru, M. Izumi, and K. Miyano, *Phys. Rev. B* **71**, 060403(R) (2005).
- ¹⁸L. C. Infante, F. Sánchez, J. Fontcuberta, M. Wojcik, E. Jedryka, S. Estradé, F. Peiró, J. Arbiol, V. Laukhin, and J. P. Espinós, *Phys. Rev. B* **76**, 224415 (2007).
- ¹⁹Z. Fang, I. V. Solovyev, and K. Terakura, *Phys. Rev. Lett.* **84**, 3169 (2000).
- ²⁰T. Z. Ward, J. D. Budai, Z. Gai, J. Z. Tischler, L. F. Yin, and J. Shen, *Nat. Phys.* **5**, 885 (2009).
- ²¹H. Boschker, M. Mathews, E. P. Houwman, H. Nishikawa, A. Vailionis, G. Koster, G. Rijinders, and D. H. A. Blank, *Phys. Rev. B* **79**, 214425 (2009).
- ²²A. Vailionis, H. Boschker, E. Houwman, G. Koster, G. Rijinders, and D. H. A. Blank, *Appl. Phys. Lett.* **95**, 152508 (2009).
- ²³S. Dong, S. Yunoki, X. Zhang, C. Sen, J.-M. Liu, and E. Dagotto, *Phys. Rev. B* **82**, 035118 (2010).
- ²⁴C. L. Lu, X. Chen, S. Dong, K. F. Wang, H. L. Cai, J.-M. Liu, D. Li, and Z. D. Zhang, *Phys. Rev. B* **79**, 245105 (2009).
- ²⁵R. W. Li, H. B. Wang, X. W. Wang, X. Y. Yu, Y. Matsui, Z. H. Cheng, B. G. Shen, E. W. Plummer, and J. D. Zhang, *Proc. Natl. Acad. Sci. U.S.A.* **34**, 14224 (2009).